Homo- and heteroanionic alkali metal aza-enolate aggregates derived from *o*-methylvalerolactim ether†‡

Philip C. Andrews,*[a] Steven D. Bull[b] and Magdaline Koutsaplis[a]

Received (in Montpellier, France) 3rd February 2010, Accepted 3rd May 2010
DOI: 10.1039/c0nj00088d

The reaction of *o*-valerolactim ether with BuM (M = Li, Na, K) in the presence of the Lewis donors thf, tmeda, pyridine and pmdta resulted in the crystallisation and structural characterisation of a series of homo- and heteroanionic aggregates, which are also either homo or heterobimetallic. All the structures incorporate an aza-enolate (1-aza-allyl) anion (= R) derived from deprotonation of the lactim ether at the α-C, and its subsequent electronic rearrangement such that the metal bonds to the amido N. Lithiation resulted in crystals of $[R_3\{R(Me_2SiO)\}Li_4\cdot(thf)_4]$, **1**, with Me_2SiO^- incorporated from the base induced decomposition of silicone grease; the linked dimer $[R_4Li_4\cdot(tmeda)_3]$, **2**, which has both terminal and bridging tmeda molecules; the octanuclear cluster $[R_6{-}\mu^6\text{-}O{-}Li_8\cdot(pyr)_2]$, **3**, which is constructed around an O^{2-} anion; and $[R(CH_2{=}CHO)_2Li_3\cdot pmdta]_2$, **4**, which incorporates lithium ethenolate, the base induced decomposition product of thf. Sodiation resulted in crystals of the simple dimeric complex $[RNa\cdot tmeda]_2$, **5**, while potassiation resulted in the heterobimetallic cluster $[R(MeO)KLi\cdot(tmeda)]_4$, **6**, incorporating a MeO^- anion due to its nucleophilic displacement from the valerolactim ether as MeOK by ^{n}Bu and subsequent anion exchange with ^{t}BuOLi. Solution NMR studies on the reaction between RH and ^{t}BuLi in the absence of a Lewis donor revealed that both the rate of deprotonation at the α-carbon and nucleophilic substitution of the ether functionality decrease substantially. The cyclic 2-^{t}Bu-imine, as the thermodynamic product, becomes the dominant product, indicating that a Lewis donor solvent is necessary for efficient deprotonation to occur.

Introduction

Lactim ethers (aka cyclic imino ethers) constitute a highly versatile and important class of precursors in organic synthesis, particularly in the formation of biologically active heterocyclic compounds,[1] with recent examples including the synthesis of quinolizidine[2] and indolizidine[3] alkaloids. While several synthetic methods are available for modifying the basic cyclic framework of the lactim ether, two of the most important utilise lithium and magnesium organometallic reagents in promoting direct alkylation through nucleophilic substitution of the ether functionality, or electrophilic substitution of a metallated aza-enolate complex.[4–6] However, one major problem with the approach is that three competing reactions are known to occur: monoalkylation, dialkylation and deprotonation, with the synthetic outcomes dependent on the basicity and steric nature of the organometallic reagent, as well as the choice of solvent medium and reaction temperature. Grignard reagents favour nucleophilic displacement and the formation of mono and dialkylated products in low to moderate yield, as do organolithium reagents when the reactions are conducted in Et_2O at −24 °C.[5] Selective deprotonation can be achieved in thf at −78 °C with lithium diisopropylamide (LDA), a weak nucleophile, but only for the six-membered lactim ether, *o*-methylvalerolactim. However, this did allow for the synthesis of α-substituted lactim ethers in poor to moderate yields through treatment of the proposed lithiated intermediate with various electrophiles.[4]

On reinvestigating these reactions with the purpose of establishing the most suitable conditions for deprotonation and alkylation, we recently reported that both ^{t}BuLi and ^{n}BuLi are effective bases for the deprotonation of *o*-methylvalerolactim when used in thf at −78 °C, if followed by warming to 0 °C prior to the addition of the electrophile, again at −78 °C. This procedure allowed us to prepare and describe a new high yielding synthetic strategy for the formation of α-alkyl-δ-amino esters and α-alkyl-valerolactams.[6]

Earlier work on the lithiation of the closely related Schöllkopf's bis-lactim ether established that the metallated intermediates adopt an aza-enolate conformation in both the solid and solution states,[7,8] though the presence of a Lewis donor is required to promote the carbanion to amide rearrangement. In contrast, there have been no reports on the structural chemistry of the organometallic intermediates formed by the structurally more simple lactim ethers, as represented by *o*-methylvalerolactim ether, though it is commonly postulated that alkylation at the α-position is preceded by the formation of a stable aza-enolate intermediate (Scheme 1).

[a] *School of Chemistry, Monash University, PO Box 23, Clayton, Melbourne, Vic. 3800, Australia. E-mail: phil.andrews@sci.monash.edu.au; Fax: +61 3 9905 4597; Tel: +61 3 9905 5509*
[b] *Department of Chemistry, University of Bath, Bath, UK BA2 7AY*
† This article is part of a themed issue on Main Group chemistry.
‡ CCDC reference numbers 764914–764919. For crystallographic data in CIF or other electronic format see DOI: 10.1039/c0nj00088d

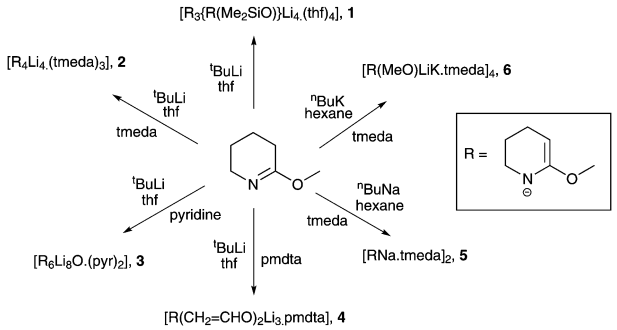

Scheme 1 Reactions of *o*-methylvalerolactim ether with BuM (M = Li, Na, K) in the presence of various Lewis donors, and identified crystalline reaction products **1–6**. Various reaction conditions are reported in Experimental section.

In this paper we now report the results of our study into the metallated intermediates obtained on treating *o*-methylvalerolactim ether with BuM (M = Li, Na, K) in both the presence and absence of various Lewis base donors: thf, tmeda, pmdta and pyridine. The heavier alkali metal complexes were used to establish the effect of increased basicity on the nature of the anionic intermediate in the knowledge that both Na^+ and K^+ can promote both structural and electronic rearrangements in such anions.

We have found that simple metallated valerolactim ethers, after adopting an aza-enolate (or 1-aza-allyl) configuration, are reluctant to form solid complexes in the presence of common Lewis donor solvents; the exception being the bidentate donor tmeda. Crystallisation generally occurs when a second anion can be incorporated, and hence gives rise to a panoply of fascinating heteroanionic complexes which are either homometallic or heterobimetallic. The solid state elucidation of such aggregated complexes is not common, though they are highly sought after since they are structurally linked to the highly reactive, unusually selective and often elusive 'superbase' complexes.

As such, we now report the first isolated and characterised lithiated aza-enolate derivatives of *o*-methylvalerolactim: $[R_3\{R(Me_2SiO)\}Li_4{\cdot}(thf)_4]$, **1** (where R = $C_6H_{10}NO$, the aza-enolate form of *o*-methylvalerolactim), which has incorporated Me_2SiO^-, a common decomposition product of silicone grease; $[R_4Li_4{\cdot}(tmeda)_3]$, **2** (tmeda = *N*,*N*,*N*′,*N*′-tetramethylethylenediamine); the octanuclear cluster $[R_6{-}\mu^6{-}O{-}Li_8{\cdot}(pyr)_2]$, **3** (pyr = pyridine), constructed around an O^{2-} anion; and $[R(CH_2{=}CHO)_2Li_3{\cdot}pmdta]_2$, **4** (pmdta = *N*,*N*′,*N*′,*N*″,*N*″-pentamethyldiethylenetriamine), which has incorporated lithium ethenolate, the base induced decomposition product of thf. Sodiation gave the dimeric complex $[RNa{\cdot}tmeda]_2$, **5**, while potassiation resulted in the heterobimetallic cluster $[R(MeO)KLi{\cdot}(tmeda)]_4$, **6**, which includes a MeO^- anion arising from nucleophilic displacement from the valerolactim ether and subsequent anion exchange with ^{t}BuOLi.

Results and discussion

Syntheses

While both ^{n}BuLi and ^{t}BuLi deprotonate *o*-methylvalerolactim at the α-C, ^{t}BuLi was used preferentially in our study since it produces the desired α-alkylated product in the highest yield.[6] All reactions were conducted at low temperature and crystallisation was mainly attempted in low polarity solvents, such as hexane and toluene, due to the higher solubility and increased reactivity of alkali metal organyls in, and towards, more polar solvents. In addition to thf, the lithiated lactim ethers were treated with pyridine, tmeda and pmdta. Reactions conducted in the absence of any Lewis base are described in a later section. Only the tmeda complexes of Li and Na could be precipitated and isolated as crystalline solids. All other complexes appear to be oils and could not be precipitated, even on storage over solid CO_2. Crystals that were obtained from the reaction mixtures had incorporated various unanticipated anions; Me_2SiO^-, MeO^-, $CH_2{=}CHO^-$ and O^{2-}, highlighting the highly reactive nature of the organometallic reactants and products.

The isolated crystalline products were analysed where possible by multinuclear and variable temperature NMR, single crystal X-ray diffraction, and by elemental analysis. However, obtaining consistent elemental analysis proved very challenging and acceptable results were not always achieved. The various reactions and their products are summarised in Scheme 1.

Lithiation of lactim ethers, and their subsequent modification with electrophiles, is normally conducted in thf at low temperatures. As such, the first target was to obtain insights into the nature of the complex formed in this solvent. The addition of ^{t}BuLi to *o*-methylvalerolactim in thf at −78 °C results in the gradual formation of a bright yellow solution as the reaction mixture warms to room temperature over a 2 h period. Removal of the volatile solvents *in vacuo* leaves only a viscous yellow oil, which can be solubilised in hexane. Typically, no solid product can be coaxed from this solution. However, on one occasion, storing the solution at 2 °C over several days produced a small crop of prismatic colourless crystals. These crystals were identified as $[R_3\{R(Me_2SiO)\}Li_4{\cdot}(thf)_4]$, **1**, having incorporated a Me_2SiO^- anion through the base induced decomposition of silicone grease. Silicone grease (polydimethylsiloxane) consists of linear repeating units of $-Me_2SiO^-$ terminated by SiOH. Its decomposition is relatively common and is known to occur in hydrocarbon solvents in the presence of organometallic bases, particularly those of the s block metals.[9] Consequently the Me_2SiO^- anion has a tendency of inserting into polar bonds, as is found in complex **1**. The reactivity of polydimethylsiloxane and the possible mechanism by which insertion of Me_2SiO^- occurs has been reviewed.[9] Attempts to replicate **1** following the deliberate addition of silicone grease were not successful.

Tmeda is commonly used in organolithium chemistry to enhance both reactivity and reaction rates through chelation and deaggregation,[10–12] and can be competitive with thf in bonding with Li. As such, one equivalent of tmeda was added to the thf based yellow reaction mixture at room temperature. On removing the volatiles *in vacuo* a pale yellow solid remained. Solubilising the solid in hexane and storing the yellow solution at 2 °C produced a crop of pale yellow prismatic crystals. These were characterised as $[R_4Li_4{\cdot}(tmeda)_3]$ **2**. Thus, stoichiometric addition of tmeda has displaced coordinating thf, in a thf solution. In comparison, the stoichiometric

addition of thf to $[\{(^{i}Pr)_2NLi\}_2{\cdot}(tmeda)_3]$, the predominant solution species of LDA in the presence of tmeda, readily displaces tmeda forming the thf solvate.[12] This would suggest that the aggregate formed by complex **2** is more thermodynamically stable than the thf solvate.

Pyridine, a nitrogen based monodentate donor, was added to the thf based reaction mixture when it had warmed to −20 °C, and was subsequently left to warm to room temperature. Removing all the volatile components *in vacuo* left a viscous orange oil. Taking this oil up in hexane and storing the orange solution at room temperature (*ca.* 22 °C) for seven days produced a crop of colourless cubic crystals. These crystals were identified as $[R_6{-}\mu^6\text{-}O{-}Li_8{\cdot}(pyr)_2]$ **3**. Group 1 organometallic compounds are strongly reactive towards O_2 and H_2O.[13] The source of O^{2-} in previously characterised Li amide complexes has been identified as being predominantly from H_2O, incorporating the oxide anion as Li_2O.[13–15] From ^1H NMR analyses of reagents and solvents, the source of H_2O appears to be primarily from thf collected and used directly from the solvent purification system (SPS). The reaction was repeated using thf that had been extracted from the SPS and subsequently dried thoroughly by reflux over Na wire, and collected by distillation. On repeating the synthetic procedure described above, no solid product could, under these conditions, be coaxed from the hexane solution. Eventual removal of all volatiles left only a viscous orange oil consistent with other attempts at crystallising the mono-anionic $[RLi(L)_k]_n$ complexes.

The addition of Lewis base donors of higher denticity, such as pmdta, tends to maximise deaggregation, with a large number of organolithium monomers isolated and characterised as pmdta solvates.[16–20] On this occasion one equivalent of pmdta was added at 0 °C and the solution left to stir at ambient temperature for 30 min. Removal of all the volatile components *in vacuo* again resulted only in a viscous orange oil, which was solubilised in hexane. Storage of this solution at −24 °C over a three week period resulted in deposition of a small crop of colourless needles which were identified as $[R(CH_2{=}CHO)_2Li_3{\cdot}pmdta]_2$, **4**. The inclusion of lithium ethenolate, the lithium enolate of acetaldehyde ($CH_2{=}CHOLi$), derives from the base induced decomposition of thf.[21] The half-life for ^{t}BuLi in thf is 100 h at −100 °C[22] and so even though the addition of ^{t}BuLi was conducted at −78 °C, there has been competitive decomposition of thf as the reaction warmed, and possibly on subsequent storage at room temperature. This suggests that deprotonation of the lactim ether is not a rapid or fully complete reaction, since it is unlikely that the aza-enolate complex was responsible for cleaving thf since it is a much weaker base. A more direct and deliberate synthesis was attempted through the addition of the preformed lithium ethenolate to the lithium aza-enolate complex, while a second involved the deliberate decomposition of a thf solution with ^{t}BuLi and its addition to a solution of lithium aza-enolate. Unfortunately, each attempt was not successful in obtaining a solid product which characterised as **4**.

In contrast to the lithiation reactions, sodiation of *o*-methylvalerolactim was carried out using a suspension of ^{n}BuNa in hexane at 0 °C to avoid cleavage of thf which can happen even at very low temperatures. Sodiation resulted in the formation of a yellow precipitate, which was subsequently solubilised through the addition of one equivalent of tmeda. The solution was filtered, with storage at 2 °C resulting in the deposition of a crop of pale yellow needles. These crystals were identified as $[RNa{\cdot}tmeda]_2$, **5**.

^{n}BuK also readily cleaves thf even at temperatures as low as −100 °C,[23] and consequently potassiation of *o*-methylvalerolactim using ^{n}BuK was carried out in hexane at −60 °C. One equivalent of tmeda was added to the dark red suspension resulting in the dissolution of the majority of the precipitate. The solution was filtered at room temperature and storage of the filtrate at 2 °C for *ca.* five days resulted in the deposition of a small crop of orange crystals. These crystals were identified as $[R(MeO)KLi{\cdot}tmeda]_4$, **6**, incorporating an equivalent of lithium methoxide. This most likely originates from an impurity in the ^{n}BuK. The synthesis of ^{n}BuK involves the addition of ^{n}BuLi to a ^{t}BuOK suspension in hexane, resulting in the precipitation of ^{n}BuK.[24] The hexane soluble ^{t}BuOLi by-product is generally removed through washing the ^{n}BuK precipitate with several aliquots of hexane. It is assumed in this instance that some residual ^{t}BuOLi impurity has persisted in the ^{n}BuK, and that the source of the MeO^- group is from the nucleophilic substitution of *o*-methylvalerolactim by ^{n}BuK. Anion exchange (MeOH being the stronger acid) provides the source of MeOLi. No other solid material appeared from the filtrate. Unfortunately, the crystals of **6** readily decompose when solvent is removed *in vacuo*. Several attempts were made to deliberately synthesise **6**, including the deliberate addition of a ^{t}BuOK/^{n}BuLi mixture to *o*-methylvalerolactim followed by tmeda. None were successful, illustrating once again the high degree of serendipity involved in obtaining crystals of heteroanionic and heterobimetallic complexes. Consequently, the only characterisation obtained was by single crystal X-ray crystallography.

Solid-state structures

The crystal structures obtained for all complexes **1–6** indicate certain common key structural features; deprotonation occurs at the α-C of the lactim ether, resulting in formation of η^1-aza-enolate anions, and migration of the metal to form more stable $M{-}N_{amido}$ bonds. Given the complexity of each structure they are described below in-turn.

$[R_3\{R(Me_2SiO)\}Li_4{\cdot}(thf)_4]$, 1. Complex **1**, $[R_3\{R(Me_2SiO)\}Li_4{\cdot}(thf)_4]$, crystallises in the triclinic space group $P\bar{1}$, and is composed of four independent units giving a *pseudo* tetrameric structure. The structure is shown in Fig. 1. The disruptive feature, possibly preventing higher symmetry and formation of a genuine tetramer, is the insertion into one Li–N bond of dimethylsilylanone, Me_2SiO^-.

The complex contains formal $Li{-}N_{amido}$ bonds in the range 1.967(3) to 2.064(3) Å (Table 1). These are comparable to those in previously characterised σ-bonded Li amides[17,25–27] and also in the related lithiated Schöllkopf's bis-lactim ethers, ranging from 1.965(3) to 2.089(5) Å.[7,8] Each methoxy group acts as an internal donor, binding to a different Li cation to that of its corresponding N. The $Li{-}O_{Me}$ bond distances range from 1.975(3) to 2.059(3) Å, which is within the expected range of Li–O dative bonds.[8,28] This compares well with the chiral Li

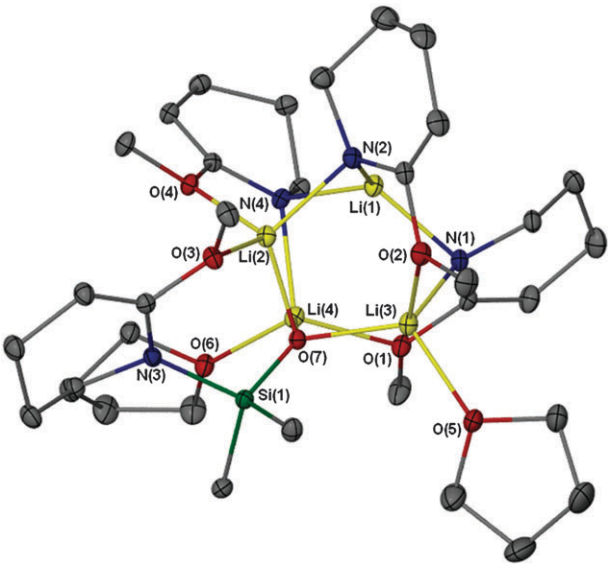

Fig. 1 Solid-state structure of complex **1**, with all hydrogen atoms omitted for clarity. Thermal ellipsoids are shown at the 30% probability level.

Table 1 Selected bond lengths (Å) present in complex **1**

Bond	Length	Bond	Length	Bond	Length
Li(1)–N(1)	1.967(3)	Li(3)–N(1)	2.056(3)	N(1)–C(5)	1.348(2)
Li(1)–N(2)	1.975(3)	Li(3)–O(2)	2.043(3)	C(4)–C(5)	1.357(2)
Li(1)–N(3)	1.976(3)	Li(3)–O(5)	2.017(3)	N(2)–C(11)	1.358(2)
Li(2)–N(2)	2.006(3)	Li(3)–O(7)	1.923(3)	C(10)–C(11)	1.348(3)
Li(2)–O(3)	1.995(3)	Li(4)–N(4)	2.065(3)	N(3)–C(17)	1.385(2)
Li(2)–O(4)	1.975(3)	Li(4)–O(1)	2.059(3)	C(16)–C(17)	1.335(2)
Li(2)–O(7)	1.927(3)	Li(4)–O(6)	2.035(3)	N(4)–C(23)	1.361(2)
		Li(4)–O(7)	1.910(3)	C(22)–C(23)	1.348(2)

aza-enolate complex Li–2-acetylnaphthalene–SAMP–hydrazone (SAMP = (*S*)-1-amino-2-methoxymethylpyrrolidine), which has an internal solvating methoxy group with a Li–O bond length of 1.982(3) Å.[29] Due to this internal solvation, only two thf molecules are incorporated into the 'tetrameric' structure. A similar phenomenon is observed in the lithiated Schöllkopf's bis-lactim ether complex, 1-lithio-3,6-diethoxy-2,5-dimethyl-1,2-dihydropyrazine,[7] in which only one thf molecule is coordinated to the Li cation due to internal coordination by two ethoxy groups.

The formation of the aza-enolate anion is characterised by N–C and C–C bond lengths ranging 1.348(2)–1.385(2) and 1.335(2)–1.357(2) Å respectively (Table 1). The magnitude of the bond lengths indicates a delocalisation of charge along N⩵C⩵C.

The bond lengths are interposed between isolated non-cyclic lithium aza-enolate structures (N⩵C⩵C of 1.369(2) and 1.372(2) Å)[29] and Schöllkopf's bis-lactim ethers (N(1)–C(1) 1.36(1) and C(1)–C(2) 1.36(1) Å),[7] though in the latter the second double bond allows for greater charge delocalisation. In comparison to delocalised aza-enolate structures, enamines generally have C–N and C=C bonds of *ca.* 1.40 and 1.34 Å respectively.[30] The ligand which is affected by the insertion of Me_2SiO^-, thereby generating a silylamide, more closely resembles a cyclic enamine (N(3)–C(17) 1.385(2) and C(17)–C(16) 1.335(2) Å), than an aza-enolate anion. The bond between C(17)–O(3) is also slightly shorter (1.380(2) Å) compared to that of 1.406(2) Å for the remaining aza-enolate ligands.

Table 2 Selected bond angles (°) in complex **1**

Bond	Angle	Bond	Angle
N(1)–Li(1)–N(2)	114.9(2)	N(1)–Li(3)–O(5)	108.2(1)
N(1)–Li(1)–N(4)	116.5(2)	N(1)–Li(3)–O(2)	104.0(2)
N(2)–Li(1)–N(4)	116.1(2)	O(2)–Li(3)–O(7)	105.8(1)
N(2)–Li(2)–O(4)	105.3(2)	O(7)–Li(3)–N(1)	114.2(2)
O(4)–Li(2)–O(7)	114.5(2)	N(4)–Li(4)–O(6)	103.6(1)
O(4)–Li(2)–O(3)	107.4(1)	N(4)–Li(4)–O(1)	105.9(1)
O(7)–Li(2)–N(2)	116.8(2)	O(6)–Li(4)–O(7)	116.0(2)
		O(7)–Li(4)–N(4)	110.7(2)

Each Li cation is unique, with two distinct coordination environments for the four Li atoms. Li(1) is formally three coordinate binding to three N_{amido} with a coordination geometry close to trigonal planar; angles ranging from 114.9(2) to 115.5(2)° (Table 2). The three remaining Li cations are four coordinate, each binding to one N_{amido} and three O centres. The structural implication of the inserted Me_2SiO^- moiety is evident, with all three Li cations binding to the dimethylsilylanone oxygen.

The lack of symmetry in the structure makes it difficult to classify it within the ring laddering or ring stacking structural domains.[31] It possesses two distorted Li–N–C–O–Li–N six-membered rings and a search of the CSD reveals no analogous reported structure. At an initial glance, complex **1** appears to consist of two stacked distorted six-membered rings linked by two Li–N bonds and one Li–O bond, though the fourth link comprises of N(4)–C(23)–O(4)–Li(2) atoms, which does not exemplify the formation of the ring stacking motif.

$[R_4Li_4{\cdot}(tmeda)_3]$, 2. Complex **2**, $[R_4Li_4{\cdot}(tmeda)_3]$, crystallizes in the monoclinic space group $P2_1/n$ as a dimer with crystallographically imposed inversion symmetry. The structure is shown in Fig. 2. The two $[R_2Li_2{\cdot}(tmeda)_{1.5}]$ units are linked by a single η^1-tmeda molecule and terminated by two chelating tmeda molecules. A crystallographic inversion centre is located in the midpoint of the bridging tmeda molecule. As expected, the ligand is deprotonated at the α-C forming an η^1-aza-enolate complex, with formal N–Li bonds that range from 2.002(6) to 2.075(5) Å (Table 3). The bonds that

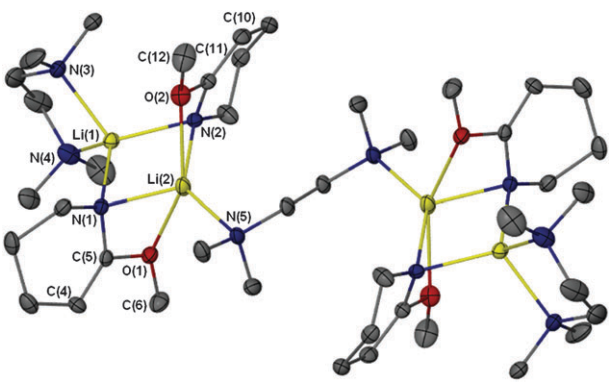

Fig. 2 Solid-state structure of complex **2**, with all hydrogen atoms omitted for clarity. Thermal ellipsoids are shown at the 30% probability level.

Table 3 Selected bond lengths (Å) and angles (°) present in complex **2**

Bond	Length	Bond	Length	Bond	Angle
Li(1)–N(1)	2.067(5)	N(1)–C(5)	1.357(4)	N(1)–Li(1)–N(2)	104.5(2)
Li(1)–N(2)	2.075(5)	C(4)–C(5)	1.347(4)	N(1)–Li(1)–N(3)	120.9(3)
Li(1)–N(3)	2.155(5)	N(2)–C(11)	1.343(3)	N(1)–Li(1)–N(4)	112.5(2)
Li(1)–N(4)	2.202(5)	C(10)–C(11)	1.352(4)	N(3)–Li(1)–N(4)	83.0(2)
Li(2)–N(1)	2.033(6)			N(1)–Li(2)–N(2)	108.6(2)
Li(2)–N(2)	2.002(6)			N(1)–Li(2)–O(1)	59.9(2)
Li(2)–N(5)	2.113(5)			N(1)–Li(2)–N(5)	118.3(3)
Li(2)–O(1)	2.376(6)			Li(1)–N(1)–Li(2)	73.2(2)
Li(2)–O(2)	2.388(6)			Li(1)–N(2)–Li(2)	73.6(2)

characterise the aza-enolate complex are N(1)–C(5) 1.357(4), C(4)–C(5) 1.347(4), N(2)–C(11) 1.343(3) and C(10)–C(11) 1.352 Å. It is evident that there is agreement in the bond lengths between complex **1** (*cf.* N–C 1.348(2) to 1.361(2) Å and C–C 1.348(3) to 1.352(2) Å) and complex **2**.

There are two distinct coordination environments for the Li cations. Li(1) is formally four co-ordinate binding to four N in a distorted tetrahedral geometry, with cation centred angles ranging from 104.5 to 120.9°, which are comparable to other solvated Li amide dimers.[26,32,33] In comparison to Li(1) in **1** (*cf.* 1.967(3) to 2.064(3) Å), the Li–N bonds in **2** are slightly longer (2.002(6) to 2.075(5) Å), most likely due to the higher coordination number of Li(1) in **2**. Li(2) is formally five coordinate binding to three N: including two aza-enolate ligands and one N of the bridging tmeda molecule. Li(2) lies almost centrally between both N–C–O moieties, interacting with both the C and O atoms of the aza-enolate anion, characterised by the bond lengths Li(2)–C(5) 2.590(6); Li(2)–O(1) 2.376(6); Li(2)–C(11) 2.616(6) and Li(2)–O(2) 2.388(6) Å. Each aza-enolate moiety can be considered as chelating to Li(2). The tmeda chelating angle around Li(1) is 83.0(2)°. This leads to the unusual structural feature of two terminally chelating tmeda molecules and one that bridges the two dimeric units. The interaction of Li(2) with the N–C–O motif of the aza-enolate complex results in a sterically crowded environment making it more energetically favourable for the chelating tmeda to flip around and act as a bridge between the two dimers.

Interestingly, studies on the structural chemistry of LDA with common Lewis bases indicate that η^1-binding of tmeda to a dimeric LDA unit is the preferred bonding mode rather than chelation.[12] In fact, this is observed in the solid-state structure of $[(^i\mathrm{Pr})_2\mathrm{NLi}\cdot\mathrm{tmeda}]_\infty$. However, it was found that thf can readily displace the monodentate tmeda molecules, in contrast to what is observed in **2**.

Li(1) is not involved in any additional interactions and therefore tmeda is able to chelate to the Li centre. A search of the literature reveals only one other lithium organonitrogen complex with the same bonding motif of having two chelated dimers linked by an η^1-tmeda molecule.[34] However, it is slightly more common for organolithium (C–Li) complexes.[35]

$[R_6$–μ^6-O–$Li_8\cdot(pyr)_2]$, 3. Complex **3**, $[R_6$–μ^6-O–$Li_8\cdot(pyr)_2]$, crystallises in the triclinic space group $P\bar{1}$ as a centro-symmetric Li_8 cluster with a μ^6-O^{2-} core. The structure is shown in Fig. 3. The aza-enolate anion has bond lengths N(1)–C(5) 1.365(3), C(4)–C(5) 1.339(3), N(2)–C(11) 1.360(3),

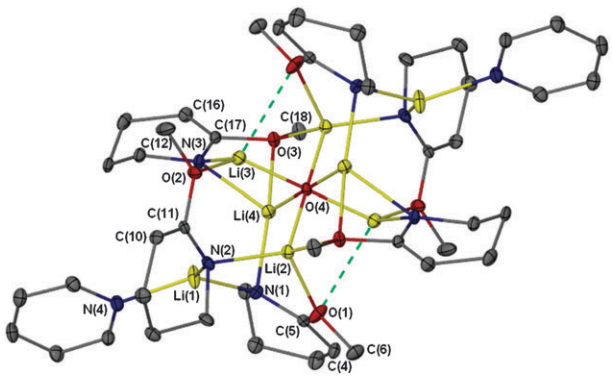

Fig. 3 Solid-state structure of complex **3**, with all hydrogen atoms omitted for clarity. Thermal ellipsoids are shown at the 30% probability level.

C(10)–C(11) 1.337(3), N(3)–C(17) 1.356(3) and C(16)–C(17) 1.342(3) Å (Table 4) which, in comparison with **2**, indicate a lower degree of delocalisation and greater C=C bond character. This may be a consequence of the inclusion of the highly electronegative O^{2-} centre, with the electropositive Li centres not as effective in inducing delocalisation.

The coordination environment around each Li is similar to that in complex **1**, with four unique Li centres and two coordinating pyridine molecules, analogous to the two coordinated thf molecules. Li(1) is formally three coordinate, with close to trigonal planar geometry, angle range 116.8(2)–119.6(2)° (Table 5), through binding to three N; two N_{amido} and one N from a coordinated pyridine molecule. Li(2) possesses a *pseudo* tetrahedral geometry binding to one N_{amido} and three O. Li(4) is four coordinate binding to two N_{amido} and two O, unlike in complex **1** where it is binding to one N_{amido} and three O atoms. As in complex **1**, each methoxy group bonds to a different Li centre to its corresponding N, except for Li(4) which is bonded to a methoxy group and N_{amido} from the same aza-enolate ligand. In terms of other

Table 4 Selected bond lengths (Å) present in complex **3**

Bond	Length	Bond	Length	Bond	Length
Li(1)–N(1)	1.990(5)	Li(3)–N(3)	2.004(5)	N(1)–C(5)	1.365(3)
Li(1)–N(2)	2.010(5)	Li(3)–O(2)	1.931(4)	C(4)–C(5)	1.339(3)
Li(1)–N(4)	2.049(5)	Li(3)–O(4)	1.847(4)	N(2)–C(11)	1.360(3)
Li(2)–N(2)	2.023(4)	Li(3)–O(1)$^{\#}$	2.668(5)	C(10)–C(11)	1.337(3)
Li(2)–O(1)	1.967(4)	Li(4)–O(4)	1.830(4)	N(3)–C(17)	1.356(3)
Li(2)–O(4)	1.860(4)	Li(4)–N(1)$^{\#}$	1.996(5)	C(16)–C(17)	1.342(3)
Li(2)–O(3)$^{\#}$	2.096(4)	Li(4)–N(3)$^{\#}$	2.089(4)	Li(4)–O(3)*	2.087(4)

Table 5 Selected angles (°) present in complex **3**

Bond	Angle	Bond	Angle
N(1)–Li(1)–N(2)	119.6(2)	N(1)$^{\#}$–Li(4)–O(4)	116.6(2)
N(1)–Li(1)–N(4)	119.5(2)	N(3)$^{\#}$–Li(4)–O(3)$^{\#}$	65.4(1)
N(2)–Li(1)–N(4)	116.8(2)	O(4)–Li(4)–N(3)$^{\#}$	102.1(2)
N(2)–Li(2)–O(1)	113.1(2)	O(4)–Li(4)–O(3)$^{\#}$	99.0(2)
O(4)–Li(2)–N(2)	118.9(2)	Li(2)–O(4)–Li(3)	91.2(2)
O(4)–Li(2)–O(1)	105.5(2)	Li(2)–O(4)–Li(4)	87.2(2)
O(4)–Li(2)–O(3)$^{\#}$	97.7(2)	Li(2)–O(4)–Li(4)$^{\#}$	92.8(2)
N(3)–Li(3)–O(2)	115.2(2)	Li(3)–O(4)–Li(4)	100.4(2)
N(3)–Li(3)–O(4)	104.8(2)	Li(3)–O(4)–Li(3)$^{\#}$	180.0(5)
O(4)–Li(3)–O(2)	124.7(2)		

methoxy interactions, O(1) forms an intermolecular contact with Li(3), characterised by the longer Li–O_{Me} distance of 2.668(5) Å in comparison to the other Li–O_{Me} interactions in complex **3**, which range from 1.830(4) to 2.096(4) Å. Consequently, Li(3) is formally three coordinate, although the Li(3) centred angles, which range from 104.8(2) to 124.7(2)°, resemble more closely the tetrahedral geometry around Li(2) and Li(4). This indicates that although the distance between Li(3)–O(1)$^{\#}$ is longer than the other Li–O_{Me} interactions, it is still having an evident effect on the coordination environment of Li(3).

An interesting aspect of **3** is the cage structure (Fig. 4), containing an almost octahedral μ^6-O^{2-} centre (O(4) centred angles range from 87.2(2) to 92.(8)°). This central O^{2-} ion coordinates to all the Li cations except for Li(1), which lies at the periphery of the cage structure. An analogous octahedral oxide centre is observed in the unsolvated Li_{14} cyclopentylamide cluster $[\{(c\text{-}C_5H_9)N(H)\}_{12}(O)Li_{14}]$,[14] though here the unique Li–O distance of 1.888(10) is marginally longer than the O–Li distances in **3** which range from 1.830(4) to 1.860(4) Å. Another unsolvated Li amide having a μ^6-O^{2-} Li_6 core is $[\{^nBuC(N^tBu)_2Li\}_4{\cdot}Li_2O]$.[15] Here the lower symmetry generates six different O–Li bond distances, 1.801(4) to 1.883(4) Å, and hence a more distorted octahedral geometry. There are two distinctly short O–Li bond lengths of 1.801(4) and 1.805(4), significantly shorter than the shortest O–Li bond distance in **3** being 1.340(4).

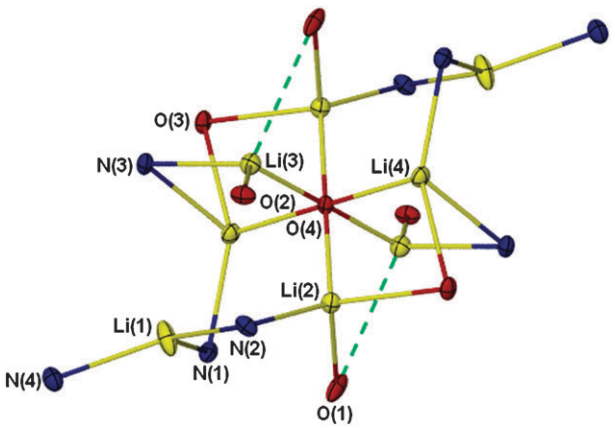

Fig. 4 Solid-state cage structure of complex **3**, with asymmetric unit labelled. All carbon and hydrogen atoms are omitted. Thermal ellipsoids are shown at the 30% probability level.

$[R(CH_2{=}CHO)_2Li_3{\cdot}pmdta]_2$, 4. Complex **4**, $[R(CH_2{=}CHO)_2Li_3{\cdot}pmdta]_2$, crystallises in the monoclinic space group *C*2/*c*. The structure contains crystallographically imposed twofold symmetry and the complete molecule is generated around a twofold axis (Fig. 5). The addition of pmdta has resulted in deaggregation, but only from a tetramer, with tmeda, to a dimer.

The incorporation of lithium ethenolate assists not only in crystallisation but in the complex adopting a ladder conformation: an established structural motif in Li amide chemistry and formed through the lateral association of $(NLi)_2$ rings.[31,36] The ladder in **4** (Fig. 6) derives from the lateral association of three four-membered rings, (NLiOLi), $(OLi)_2$ and (NLiOLi) resulting in a six rung conformation. Alternatively, the formation of complex **4** can be viewed as an association of a lithium aza-enolate monomer with the central lithium enolate dimer. Such an association is also supported by the binding

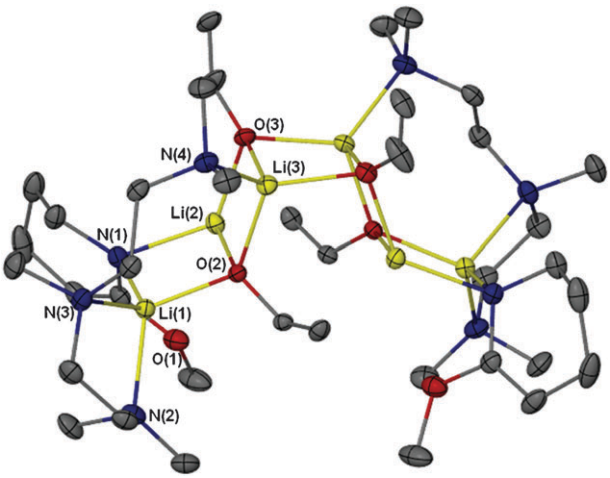

Fig. 5 Solid-state structure of complex **4**, with all hydrogen atoms omitted for clarity. Thermal ellipsoids are shown at the 30% probability level.

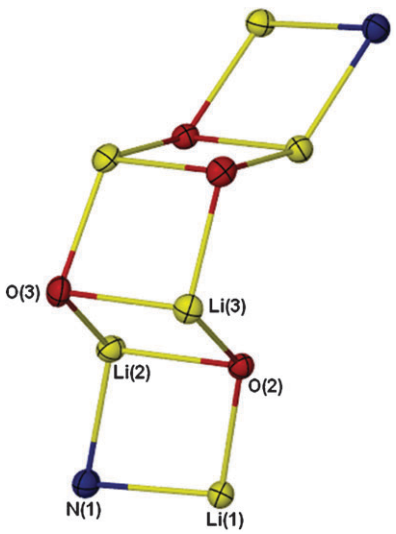

Fig. 6 Ladder structure of complex **4**. All carbon and hydrogen atoms, including pmdta molecules, are omitted. Thermal ellipsoids are shown at the 30% probability level.

mode of pmdta. In monomeric structures pmdta most often binds to the metal centre in a tridentate fashion. In complex **4** it binds to the lithium aza-enolate complex in a bidentate manner, and as a consequence of the lateral ring association bridges to the lithium enolate complex. An analogous ring composition and association has been previously observed in several other organolithium complexes: including $[(Me_2NCH_2)_3COLi{\cdot}LiNMe_2]_2$,[37] $[RNLiSiMe_2N(R)SiMe_2OLi{\cdot}(thf)_2]$ (R = 3,5-Me_2Ph, 2,6-$^iPr_2$Ph),[38] $[(CMe_3SiMe_2OCH_2CH_2CMe_2C{=}COLi)(^iPr_2NLi)]_2$[39] and $[((Me_2NCH_2)_2CHOLi)(^iPr_2NLi)]_2$.[40] In all but one example, the compound formed is a heteroleptic amide complex similar to **4**. A recurring theme in most of the published complexes is that there is some degree of chelation that appears to stabilise the ladder complexes. This either occurs *via* an ancillary ligand or, as is the case in complex **4**, *via* pmdta.

The complex displays three unique Li environments arising from the ladder conformation and incorporation of the $LiCH_2{=}CHO$ moiety (Fig. 7). Selected bond lengths and angles are given in Tables 6 and 7. Li(1) is formally four coordinate, binding to the aza-enolate and enolate moieties through the nitrogen and oxygen, with bond distances of Li(1)–N(1) 2.016(4) and Li(1)–O(2) 1.966(4) Å respectively. In addition, it is chelated by two pmdta N atoms, with Li–N bond lengths of 2.105(4) and 2.212(4) Å. This is analogous to the coordination environment of Li in the ladder complex of $[(Me_2NCH_2)_3COLi{\cdot}LiNMe_2]_2$, which comprises a multidentate amino alkoxide anion and an amide base.[37] In **4**, Li(2) is formally three coordinate binding to the aza-enolate moiety

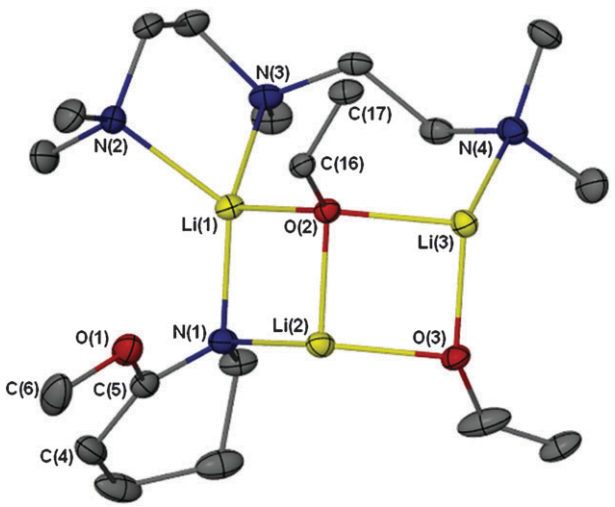

Fig. 7 Asymmetric unit of complex **4**, with all hydrogen atoms omitted for clarity. Thermal ellipsoids are shown at the 30% probability level.

Table 6 Selected bond lengths (Å) present in complex **4**

Bond	Length	Bond	Length	Bond	Length
Li(1)–N(1)	2.016(4)	Li(2)–O(3)	1.932(4)	Li(3)–O(3)$^{\#}$	1.960(4)
Li(1)–N(2)	2.105(4)	Li(2)–C(16)$^{\#}$	2.564(4)	O(2)–C(16)	1.323(2)
Li(1)–N(3)	2.212(4)	Li(2)–C(17)$^{\#}$	2.517(4)	C(16)–C(17)	1.334(3)
Li(1)–O(2)	1.966(4)	Li(3)–N(4)	2.122(4)	N(1)–C(5)	1.351(3)
Li(2)–N(1)	2.041(4)	Li(3)–O(2)	1.969(4)	C(4)–C(5)	1.350(3)
Li(2)–O(2)	1.963(4)	Li(3)–O(3)	1.964(4)		

Table 7 Selected bond angles (°) present in complex **4**

Bond	Angle	Bond	Angle
N(1)–Li(1)–N(2)	125.2(2)	N(4)–Li(3)–O(3)	117.7(2)
N(1)–Li(1)–N(3)	119.4(2)	O(2)–Li(3)–O(3)	92.6(2)
N(1)–Li(1)–O(2)	101.6(2)	Li(1)–N(1)–Li(2)	77.3(2)
N(1)–Li(2)–O(2)	100.8(2)	Li(1)–O(2)–Li(2)	80.3(2)
O(2)–Li(2)–O(3)	93.8(2)	Li(2)–O(2)–Li(3)	86.3(2)
N(4)–Li(3)–O(2)	108.7(2)	Li(2)–O(3)–Li(3)	87.3(2)

through the N_{amido} and to two enolate moieties through the oxygen atoms, with bond distances of Li(2)–N(1) 2.041(4), Li(2)–O(2) 1.963(4) and Li(2)–O(3) 1.932(4) Å respectively. The low coordination environment of Li(2) is stabilised by additional M–π interactions with the C=C bond of the enolate moiety, characterised by the short distances between Li(2)–C(16)$^{\#}$ and Li(2)–C(17)$^{\#}$ of 2.564(4) and 2.517(4) Å respectively. Li(1) and Li(3) also exhibit close contacts with enolate moiety in the magnitude of 2.7 to 2.8 Å. Li(3) is formally four coordinate binding to three enolate moieties through the oxygen atom (Li(3)–O(2) 1.969(3), Li(3)–O(3) 1.964(4) and Li(3)–O(3)$^{\#}$ 1.960(4) Å), and to a pmdta N atom (Li(3)–N(4) 2.122(4) Å), which is bridging Li(1) and Li(3).

It is interesting to note that in comparison to complexes **1–3**, the methoxy group does not bind to any lithium centre. The six membered ring of the aza-enolate moiety in **4** is orientated perpendicular with respect to the central (NLiOLi) ring, with the methoxy group sitting above the centre of the ring, characterised by the almost identical distances to Li(1) and Li(2) of 2.755 and 2.764 Å respectively. In complex **1**, the methoxy moieties are twisted toward the Li(2) cation. It would appear that the ladder conformation along with the inclusion of the lithium ethenolate has satisfied the coordination demands of the Li cations and consequently there is no need for additional coordination by the methoxy group.

While the synthesis of **4** was not easily reproduced, it should not detract the fact that the solid-state structure, as a mixed anion aggregate, is also able to function as a model for a homometallic 'superbase',[41–43] contributing to the structural chemistry available on such ubiquitous, albeit structurally elusive reagents.[44–46]

[RNa·tmeda]$_2$, 5. Complex **5**, $[RNa{\cdot}tmeda]_2$, crystallises in the monoclinic space group $P2_1/n$ as a non-centrosymmetric dimer. The structure is shown in Fig. 8. As in the lithium analogues, following deprotonation at the α-C the lactim ether rearranges to an aza-enolate anion with the sodium aza-enolate characterised by the bond distances between N(1)–C(5), C(5)–C(4), N(2)–C(11) and C(11)–C(10) of 1.357(4), 1.331(4), 1.343(4) and 1.351(4) Å respectively (Table 8).

The complex adopts a strange asymmetry. Na(1), which forms a formal Na–N bond (2.355(3) and 2.357(2) Å) with the anion, is formally four coordinate, possessing distorted tetrahedral geometry. However, it forms additional close interactions with the N=C bonds of aza-enolate moiety, characterised by the short distances between Na(1)–C(5) and Na(1)–C(11) of 3.083(4) and 3.061(4) Å respectively. In contrast, Na(2) forms longer Na–N bonds (2.475(3) and 2.480(2) Å) and with the aza-enolate moiety (Na(2)–C(5) 3.018(3) and Na(2)–C(11)

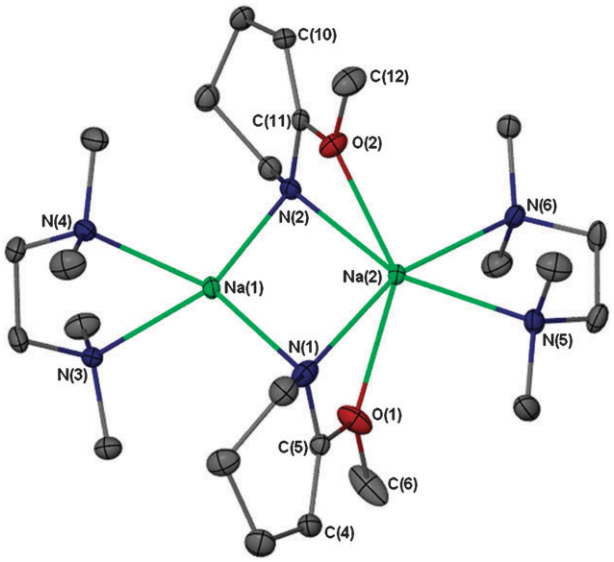

Fig. 8 Solid-state structure of complex **5**, with all hydrogen atoms omitted for clarity. Thermal ellipsoids are shown at the 30% probability level.

Table 8 Selected bond lengths (Å) present in complex **5**

Bond	Length	Bond	Length
Na(1)–N(1)	2.355(3)	Na(2)–N(6)	2.515(2)
Na(1)–N(2)	2.357(2)	Na(2)–O(1)	2.509(3)
Na(1)–N(3)	2.464(3)	Na(2)–O(2)	2.434(2)
Na(1)–N(4)	2.476(2)	Na(2)–C(5)	3.018(3)
Na(1)–C(5)	3.083(4)	Na(2)–C(11)	2.933(3)
Na(1)–C(11)	3.061(4)	N(1)–C(5)	1.357(4)
Na(2)–N(1)	2.475(3)	C(4)–C(5)	1.331(4)
Na(2)–N(2)	2.480(2)	N(2)–C(11)	1.343(4)
Na(2)–N(5)	2.529(2)	C(10)–C(11)	1.351(4)

2.933(3) Å), and in addition binds to both methoxy groups with bond distances of Na(2)–O(1) 2.509(3) and Na(2)–O(2) 2.434(2) Å (*cf.* non-bonding Na(1)–O(1) and Na(1)–O(2) distances of 3.194 and 3.090 Å respectively). The greater ligand contacts of Na(2) result in the Na(2)–$N_{aza\text{-}enolate}$ and tmeda dative bonds being slightly longer than for Na(1). The tmeda molecule that chelates to Na(1) is orientated perpendicular to the $(NNa)_2$ ring while that which chelates to Na(2) is orientated parallel to the ring, evidently minimising the steric repulsion with the coordinating methoxy groups.

Dimeric **5** possesses the paradigmatic central $(NNa)_2$ ring, observed in many previously characterised sodium amides.[47–49] The Na centred angles (107.9(1) and 100.5(1)°) in **5** are obtuse and the N centred angles (75.8(1) and 75.7(1)°) are acute (Table 9). It is noteworthy that another effect of the increased coordination number of Na(2) is that the chelating angle of tmeda is reduced by almost 4° compared to Na(1). Consequently, the aggregation state of complex **2** is further clarified. The larger ionic radius of Na in complex **5** means it is better suited in stabilising a higher coordination number, and as a consequence both tmeda molecules chelate to each Na centre. In complex **2**, $[R_4Li_4(tmeda)_3]$, the smaller coordination sphere of the Li cation means that it is not able to accommodate the increased coordination and consequently the second tmeda binds in an η^1-fashion.

Table 9 Selected bond angles (°) present in complex **5**

Bond	Angle	Bond	Angle
N(1)–Na(1)–N(2)	107.9(1)	N(1)–Na(2)–O(2)	97.3(1)
N(1)–Na(1)–N(3)	117.5(1)	N(2)–Na(2)–N(6)	92.8(1)
N(2)–Na(1)–N(3)	118.8(1)	N(5)–Na(2)–N(6)	71.2(1)
N(3)–Na(1)–N(4)	75.1(1)	N(6)–Na(2)–O(1)	112.8(1)
N(1)–Na(2)–N(2)	100.5(1)	Na(1)–N(1)–Na(2)	75.8(1)
N(1)–Na(2)–O(1)	52.7(1)	Na(1)–N(2)–Na(2)	75.7(1)

[R(MeO)KLi·tmeda]$_4$, 6. Complex **6**, $[R(MeO)KLi{\cdot}tmeda]_4$, crystallises in the orthorhombic space group *Pbcn* with crystallographically imposed twofold symmetry. The complete cluster is generated around a twofold symmetry axis. As can be seen in Fig. 9, the aggregate is heterobimetallic having unexpectedly incorporated MeOLi, most likely originating from residual ^{t}BuOLi entrained as an impurity in freshly prepared ^{n}BuK.

Though only isolated in low yield complex **6** is structurally important since it contributes to a small but growing body of 'superbase' models comprising two different anions, here aza-enolate and methoxy, and two different alkali metals, Li and K. What is unusual about **6** is that while the large majority of 'superbase' models tend to incorporate alkoxide anions of greater bulk, exemplified by the ^{t}BuO$^-$ anion,[45,50,51] only a couple of examples of analogous complexes containing MeO$^-$ or EtO$^-$ anions have been reported.[41,50]

The gross structural features conform to particular bonding patterns observed in related heterobimetallic structures in which the smaller, less electropositive metal forms well ordered σ bonded polyhedra while the larger, more electropositive metals reside on the verge of the cluster engaging in longer, less localised bonding. In **6** the central core of the cluster comprises

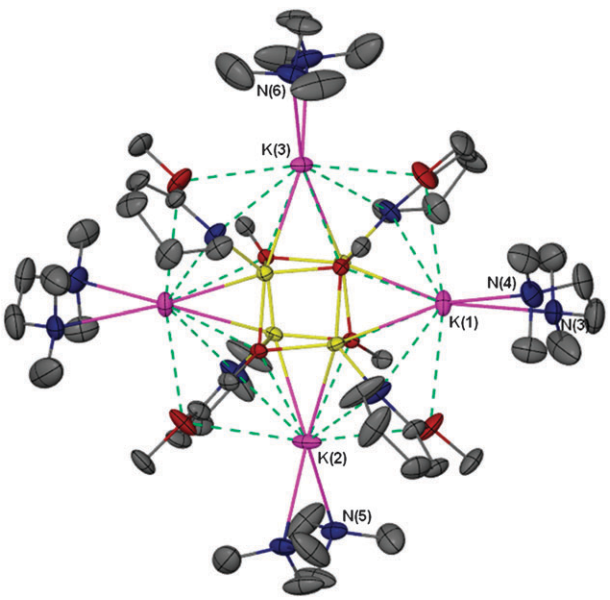

Fig. 9 Solid-state structure of complex **6**, with all hydrogen atoms omitted for clarity. Thermal ellipsoids are shown at the 30% probability level.

a σ-bonded distorted Li–O cube (Fig. 9–11), with the K cations involved in a range of less directional electrostatic interactions at the periphery. A comparison can be readily drawn with the mixed-metal (Li/K and Li/Na) complexes of *S*-*N*-α-methylbenzylallylamide (*S*-*N*-α-mba), which contain the doubly charged (N^-/C^-) anion.[42,52] Both these complexes display tetrameric aggregation, comprising a σ-bonded distorted Li–C cubane core, with the respective Na or K cations forming a $(M\cdots N)_4$ rim involving primarily π interactions. In addition, each K in **6** bonds to a single tmeda molecule, analogous to that observed for the coordination of thf to the Na cations in the Li/Na *S*-*N*-α-mba complex. This structural comparison highlights the continuity between structures of alkali metal complexes containing quite different anions. In addition, it helps validate the role of 'superbase' models in attempting to obtain a better structural and synthetic understanding of synthetically utilised 'superbases'.

Selected bond lengths and angles for **6** are given in Tables 10 and 11. Each Li cation is formally four coordinate, binding to three methoxy anions and one N of the aza-enolate, with Li–O distances ranging from 1.925(7) to 1.970(7) Å and Li–N distances of 1.941(8) and 1.950(7) Å. Li–O distances are of analogous length to those found in crystalline lithium

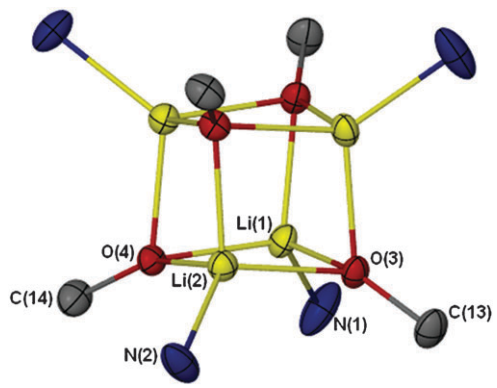

Fig. 10 Li–O cubic core present in the solid-state of complex **6**. Thermal ellipsoids are shown at the 30% probability level.

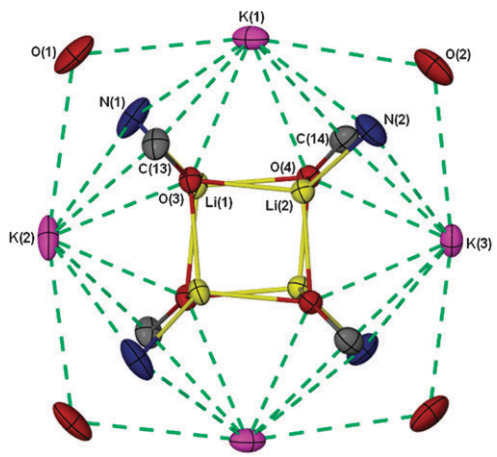

Fig. 11 Part of the solid-state structure of **6**, highlighting the K interactions. Thermal ellipsoids are shown at the 30% probability level.

Table 10 Selected bond lengths (Å) present in complex **6**

Bond	Length	Bond	Length	Bond	Length
K(1)–N(1)	3.240(5)	K(2)–O(1)	3.249(4)	Li(2)–N(2)	1.950(7)
K(1)–N(2)	3.295(4)	K(2)–O(3)	2.822(3)	Li(2)–O(3)	1.960(7)
K(1)–N(3)	2.948(4)	K(3)–N(2)	3.231(4)	Li(2)–O(4)	1.964(7)
K(1)–N(4)	2.894(5)	K(3)–N(6)	2.887(4)	Li(2)–O(4)$^{\#}$	1.925(7)
K(1)–O(1)	3.110(4)	K(3)–O(2)	3.083(4)	N(1)–C(5)	1.318(6)
K(1)–O(2)	3.229(5)	K(3)–O(4)	2.850(3)	C(4)–C(5)	1.431(4)
K(1)–O(3)	2.836(3)	Li(1)–N(1)	1.941(8)	N(2)–C(11)	1.344(6)
K(1)–O(4)	2.841(3)	Li(1)–O(3)	1.970(7)	C(10)–C(11)	1.338(7)
K(2)–N(1)	3.283(5)	Li(1)–O(4)	1.937(7)		
K(2)–N(5)	2.903(4)	Li(1)–O(3)$^{\#}$	1.944(8)		

Table 11 Selected bond angles (°) present in complex **6**

Bond	Angle	Bond	Angle
N(1)–Li(1)–O(3)	118.5(3)	N(2)–Li(2)–O(3)	121.5(4)
N(1)–Li(1)–O(4)	120.4(4)	N(2)–Li(2)–O(4)	118.7(3)
N(1)–Li(1)–O(3)$^{\#}$	122.3(4)	N(2)–Li(2)–O(4)$^{\#}$	120.8(4)
O(3)–Li(1)–O(4)	94.9(3)	O(3)–Li(2)–O(4)	94.4(3)
O(3)–Li(1)–O(3)$^{\#}$	94.7(3)	O(3)–Li(2)–O(4)$^{\#}$	99.8(3)
O(4)–Li(1)–O(3)$^{\#}$	100.0(3)	O(4)–Li(2)–O(4)$^{\#}$	95.7(3)

alkoxides, typically *ca.* 1.9 Å.[37,50] In comparison to complexes **1** to **5**, the Li–$N_{aza\text{-}enolate}$ bonds present in complex **6** are the shortest, indicating greater σ-bond character. This is most likely because the Li cations, which have distorted tetrahedral geometry, are not involved in any additional dative bonding. In comparison, each K is in a higher coordination environment, with an all inclusive coordination number of eight. The dative bonds between K and tmeda, which range from 2.887(4) to 2.948(4) Å, are shorter than the interaction evident with the aza-enolate N (3.231(4) to 3.295(4) Å), but they are within the range typical for K^+ tmeda solvates.[53,54] The K cation(s) also forms dative bonds with the methoxy moieties of *o*-methylvalerolactim, which range from 3.083(4) to 3.249(4) Å. However, it forms a closer interaction with the free methoxy anions in the central cubic core, ranging from 2.822(3) to 2.850(3) Å. The K–O bonds formed with the free methoxy are slightly longer than those in the analogous 'superbase' complex $[\{(^t\text{BuNH})(^t\text{BuO})\text{LiK}\}_4\cdot(C_6H_6)_3]$ by around 0.2 Å, although the K–N distances are in agreement.[45] Generally, complex **6** is characterised by weaker, but a larger number of, K–π interactions in comparison to fewer but stronger σ interactions in the Li core.

Solution state studies on complexes 1–5

NMR studies were conducted on complexes **1–5** and their chemical shift values compared with that of *o*-methylvalerolactim ether. Comparative values for the ^{1}H-NMR spectra obtained on the anion are compiled in Table 12. The consistent shift to higher frequency (of *ca.* 1.5 ppm) for the proton remaining on the α-C (labelled as C(OCH$_3$)C*H*), following deprotonation at that site, is indicative of the adoption by the anion of an aza-enolate conformation, and is therefore in general agreement with the bonding patterns observed in the various crystal structures. The formation of the bridging M_2–N_{amido} bonds observed in the various

Table 12 ^{1}H-NMR (C_6D_6, 30 °C) chemical shifts in ppm of anions in complexes **1–5**, compared with *o*-methylvalerolactim ether (*o*-mvl)

	Complex					*o*-mvl	
Assignment	1	2	3	4	5	Assignment	
$C(OCH_3)CH$	3.45	3.50	3.56	3.46	3.29	$C(OCH_3)CH_2$	1.92
OCH_3	3.61	3.48	3.59	3.62	3.54	OCH_3	3.63
CH_2N	3.53	3.36	3.51	3.53	3.70	CH_2N	3.42
$CHCH_2$	2.60	2.70	2.58	2.90	2.80	CH_2CH_2	1.23
$CH_2CH_2CH_2$	1.49	1.89	1.77	1.93	1.97		

solid-state aggregates is reflected in the higher frequency shifts for the CH_2 protons adjacent to the N_{amido}, indicative of greater polarisation.

While the ^{1}H-NMR spectrum of **2** obtained on the bulk solid supports the integration of the ligand to tmeda ratio to be 4 : 3, it is not definitive as to whether the bridged aggregate persists in solution. ^{1}H and ^{13}C NMR spectra at 30 °C show no distinction between the chelating and bridging tmeda molecules. In probing the possible fluxional behaviour of the bridging and terminal tmeda, variable temperature ^{1}H-NMR (400 MHz) spectra were obtained in D_8-toluene ranging from 30 °C to −80 °C in 10 °C increments. By −80 °C the ligand signals have shifted downfield (av. 0.15–0.3 ppm compared to room temperature), but only broadening of the tmeda signals is observed. If the two binding modes persist then the exchange between the chelating and bridging forms of tmeda is too rapid to be differentiated using the NMR timescale.

In the ^{7}Li-NMR spectrum at 30 °C, only one broad resonance is evident at 0.80 ppm. In attempting to differentiate between the different Li centres present in the complex a ^{7}Li-NMR spectrum was recorded in D_8-toluene at −80 °C. Four distinct resonances were observed, at 1.26, 0.97, 0.64 and 0.50 ppm, indicative of four Li cations located in four different coordination environments. This would appear to correspond with the solid-state structure in which there are four Li centres, however, only two are in different coordination environments since the complex is centro-symmetric. Thus, the ^{7}Li-NMR and ^{1}H-NMR spectra indicate an equilibrium mixture of solution species with rapid exchange in the binding modes of tmeda, and the chelating binding mode of the aza-enolate anion.

Reactivity of *o*-methylvalerolactim towards ^{t}BuLi in the absence of a Lewis donor solvent

As discussed, *o*-methylvalerolactim exhibits two different reaction pathways when reacted with organolithium reagents. Addition of ^{t}BuLi to *o*-methylvalerolactim in thf at −78 °C results in deprotonation at the α-C and formation of an aza-enolate intermediate, which can be further functionalised to an α-substituted lactim ether following addition of an electrophile.[6] Conversely, addition of ^{t}BuLi to *o*-methylvalerolactim in Et_2O at −24 °C results in nucleophilic substitution of the methoxy moiety by the ^{t}Bu group and isolation of the imine derivative.[4] Consequently, it was of interest to study the reactivity of *o*-methylvalerolactim with respect to ^{t}BuLi in the absence of any Lewis donor solvent (Scheme 2).

Addition of ^{t}BuLi to *o*-methylvalerolactim in hexane at −78 °C results in the precipitation of a pale yellow solid

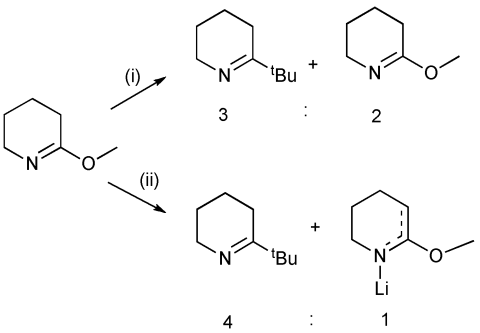

Scheme 2 Reactivity of ^{t}BuLi towards *o*-methylvalerolactim in the absence of a Lewis donor solvent. *Reaction conditions*: (i) ^{t}BuLi, thf, −78 °C to rt +30 min; (ii) ^{t}BuLi, thf, −78 °C to rt +4.5 h.

shortly after the final aliquot of ^{t}BuLi is added and the reaction allowed to begin slowly warming to room temperature. This reaction was conducted three times, and left to stir at room temperature for periods of 30 min, 1 h and 4.5 h in order to establish if the reactivity and/or selectivity is time dependent. In all instances the pale yellow solid was filtered, washed with cold hexane and analysed *via* ^{1}H-NMR and 2D-NMR (COSY) spectroscopy in C_6D_6. ^{1}H-NMR analysis following a reaction time of 30 min indicated the only reaction product to be the cyclic ^{t}Bu imine, resulting from nucleophilic displacement of MeO by ^{t}Bu, and was present alongside unreacted methylvalerolactim ether in a ratio of 3 : 2. No lithium aza-enolate product was evident. The key supporting evidence was the absence of the indicative signal at *ca.* 2.6–2.8 ppm for the β-CH_2, and while the chemical shifts for the remaining CH_2 moieties were difficult to assign, since they overlap, the sum of the integrals concurred with the number of protons present.

On increasing the reaction time to 1 h, the ^{1}H-NMR spectrum of the pale yellow solid showed subtle changes to that obtained after 30 min. A new species is apparent, characterised by two new signals at 2.59 and 4.51 ppm, suggesting the formation of the aza-enolate intermediate, although further investigation was required. As such the reaction time was extended to 4.5 h, and although the signal multiplicities were not well resolved two products were evident in 1 : 4 ratio. The 2D-NMR spectrum indicated the products to be the lithium aza-enolate complex (20%) and the cyclic ^{t}Bu imine (80%). The major difference with NMR spectra for the lithiated complexes, **1–4**, is the significant shift to higher frequency for the α-C*H*, which is now found at 4.54 ppm.

Final confirmation was obtained by quenching the pale yellow solid obtained from the 4.5 h reaction with H_2O, followed by extraction into an organic solvent, giving cyclic 2-^{t}Bu-imine and *o*-methylvalerolactim in a 4 : 1 ratio. Quenching the aza-enolate product recovers the starting lactim ether. Therefore, it would appear that in the absence of a Lewis donor solvent, nucleophilic substitution is preferred over the deprotonation pathway. At −78 °C, the kinetic deprotonation is too slow and consequently when the reaction warms to room temperature it favours the formation of the thermodynamic product. It is apparent that in the absence of a Lewis donor both the rate of deprotonation and nucleophilic

substitution decreases, which is often evident in organolithium chemistry.[21]

Conclusions

Our structural investigation into the metallated intermediates formed on reaction of *o*-methylvalerolactim ether (RH) with BuM (M = Li, Na, K) reveals that in the presence of a Lewis donor deprotonation occurs at the α-carbon with concomitant rearrangement of the anion to an aza-enolate (1-aza-allyl) complex, with metal binding to the N_{amido} centre. Solution studies revealed that in the absence of a Lewis donor solvent both the rate of deprotonation at the α-carbon and nucleophilic substitution of the ether functionality decreases substantially. Since kinetic deprotonation at −78 °C is too slow, the formation of the cyclic 2-^{t}Bu-imine, as the thermodynamic product, is favoured at room temperature. This indicates that a Lewis donor solvent is required for selective deprotonation of *o*-methylvalerolactim at the α-carbon, in addition to maintaining a low reaction temperature.

Only with tmeda as the Lewis donor were crystals of homoanionic complexes obtained; the lithiated complex being structurally characterised as $[R_4Li_4{\cdot}(tmeda)_3]$, containing both bridging and chelating tmeda, and the sodium complex as the dimer $[RNa{\cdot}tmeda]_2$, in which the anion coordinates in an asymmetric manner to the Na cations. However, potassiation resulted in the heteroanionic and heterobimetallic cluster $[R(MeO)KLi{\cdot}(tmeda)]_4$ in which MeO^- anions are incorporated after nucleophilic displacement from the valerolactim ether by ^{n}BuK, and subsequent anion exchange with ^{t}BuOLi, itself a by-product from the formation of ^{n}BuK.

No solid products could be obtained with other Lewis donors unless a heteroanionic complex was serendipitously formed. Crystals of the lithiated complexes $[R_3\{R(Me_2SiO)\}Li_4{\cdot}(thf)_4]$, $[R(CH_2{=}CHO)_2Li_3{\cdot}pmdta]_2$ and $[R_6{-}\mu^6\text{-}O{-}Li_8{\cdot}(pyr)_2]$ were isolated and characterised on inclusion of the anions Me_2SiO^-, $CH_2{=}CHO^-$ and O^{2-} in the aggregated structures. Dimethylsiloxane, Me_2SiO^-, and lithium ethenolate, $CH_2{=}CHO^-$, result, respectively, from the base catalysed decomposition products of silicone grease and thf, while O^{2-} results from adventitious moisture.

Taken as a whole, the solid state structures of these six complexes give us a valuable insight into not only the structural chemistry of the aza-enolate anion of valerolactim ether itself, but importantly into the nature of bonding in homoanionic, heteroanionic and heterobimetallic aggregates of the alkali metals, thereby shedding more light on the intriguing nature of elusive superbase-type complexes.

Experimental

General remarks

The synthetic protocols for the reactions reported herein were carried out under dry inert atmosphere conditions. All synthesis and manipulations were undertaken with the use of a vacuum/nitrogen line and Schlenk techniques and where appropriate handled in an argon glove box. Water and oxygen was removed from hexane using MBRAUN SPS-800 solvent purification system. Prior to use, thf was dried by reflux over Na, and pmdta and tmeda were dried by reflux over CaH_2. ^{n}BuLi (1.6 M in hexane) was purchased from Aldrich and standardized before use. ^{n}BuNa, ^{n}BuK and *o*-methylvalerolactim were synthesized according to the literature procedures.[24,55] ^{1}H and ^{13}C NMR spectra were recorded on a Bruker DRX 400 MHz and Bruker DRX 300 MHz spectrometer with chemical shifts referenced internally to C_6D_6. All elemental analyses were performed by CMAS, Melbourne, Australia.

Crystallography

Crystallographic data were obtained on an Enraf Nonius Kappa CCD diffractometer with graphite monochromated MoKα (λ_0 = 0.71073 Å) radiation at 123 K. All single crystals were mounted on a glass fiber under oil.[56] Data were collected and processed using the Nonius software. Structures were solved and refined by full-matrix least squares on F^2 and expanded using direct methods with all calculations performed by SHELXS 97 software[57] and X-seed interface.[58] All hydrogen atoms were placed in calculated positions (C–H = 0.95 Å) and included in the final least-squares refinement. All other atoms were located and refined anisotropically.

Syntheses and characterisation

$[R_3\{R(Me_2SiO)\}Li_4{\cdot}(thf)_4]$, 1. ^{t}BuLi (1.18 ml, 1.7 M, 2.0 mmol) was added dropwise to a stirring solution of *o*-methylvalerolactim (0.23 g, 2.0 mmol) in thf (10 ml) at −78 °C under an Ar atmosphere, the solution gradually changing from colourless to light yellow as it warmed slowly to −20 °C. At this point the solution was removed from the N_2/acetone cold bath and allowed to warm to rt. Thf was removed *in vacuo* yielding a light yellow solid, which following gentle heating was solubilised in hexane (8 ml). The yellow solution was stored at rt overnight, resulting in the deposition of colourless prismatic crystals. Yield 0.49 g, 35%. Mp 129–130 °C. δ_H (400 MHz, C_6D_6, 30 °C): δ 3.61 (5H, br s, OCH_3, OCH_2), 3.53 (2H, m, CH_2N), 3.45 (1H, m, $C(OCH_3){=}CH$), 3.42 (3H, br s, OCH_3'), 2.60 (2H, br s, $CH_2CH{=}C$), 1.85 (2H, br s, OCH_2CH_2), 1.49 (2H, br s, $CH_2CH_2CH_2$), 0.08 (6H, br s, $Si(CH_3)_2$). δ_C (100 MHz, C_6D_6, 30 °C): δ 164.2 ($C(OCH_3)$), 68.4 (OCH_2), 58.7 ($CH{=}C(OCH_3)N$), 53.8 (OCH_3), 47.1 ($CH_2CH_2CH_2$), 27.1 ($CH_2CH_2CH_2$), 24.4 ($CH_2CH{=}C$), 1.92 ($Si(CH_3)_2$).

Crystallographic data for **1**. $C_{34}H_{62}Li_4N_4O_7Si$, M = 694.73, colourless prismatic, 0.10 × 0.08 × 0.08 mm, triclinic, space group $P\bar{1}$ (No. 2), a = 10.2332(2), b = 11.2688(2), c = 17.5740(4) Å, α = 88.1390(10)°, β = 89.7480(10)°, γ = 77.4630(10)°, V = 1977.19(7) Å^3, Z = 2, D_c = 1.167 g cm^{-3}, F_{000} = 752, Nonius Kappa CCD, MoKα radiation, λ = 0.71073 Å, T = 123(2) K, $2\theta_{max}$ = 60.3°, 37 027 reflections collected, 11 494 unique (R_{int} = 0.0415). Final GooF = 1.032, R_1 = 0.0591, wR_2 = 0.1386, R indices based on 8310 reflections with $I > 2\sigma(I)$ (refinement on F^2), 457 parameters, 0 restraints. Lp and absorption corrections applied, μ = 0.107 mm^{-1}.

[R_4Li_4·(tmeda)$_3$], 2. ^{t}BuLi (1.18 ml, 1.7 M, 2.0 mmol) was added dropwise to a stirring solution of *o*-methylvalerolactim (0.23 g, 2.0 mmol) in thf (10 ml) at −78 °C under an Ar atmosphere, the colourless solution gradually changing to light yellow colour as it warmed to −20 °C. At this point the solution was removed from the N_2/acetone cold bath and allowed to warm up to rt. Tmeda (0.30 ml, 2.0 mmol) was then added slowly to the solution at 0 °C and allowed to stir for 30 min and warm to rt. During this time the solution became dark yellow in colour. Volatiles were removed *in vacuo* yielding a light yellow solid, which after gentle heating was solubilised in hexane (5 ml). The yellow solution was stored at 2 °C overnight, resulting in the deposition of clear cubic crystals. Yield 0.55 g, 67%. Mp 118–119 °C. δ_H (400 MHz, C_6D_6, 30 °C): δ 3.50 (1H, m, C(OCH$_3$)=C*H*), 3.48 (3H, s, OC*H*$_3$), 3.36 (2H, t, $^3J_{HH}$: 3.3 Hz, C*H*$_2$N), 2.70 (2H, q, $^3J_{HH}$: 3.2 Hz, C*H*$_2$CH=C), 2.11 (12H, s, N(C*H*$_3$)$_2$), 2.08 (4H, s, N(C*H*$_2$)$_2$), 1.89 (2H, m, CH$_2$C*H*$_2$CH$_2$). δ_C (100 MHz, C_6D_6, 30 °C): δ 169.0 (*C*(OCH$_3$)), 110.4 (C(OCH$_3$)=*C*H), 58.1 (N(*C*H$_2$)$_2$), 53.1 (O*C*H$_3$), 48.6 (*C*H$_2$N), 46.5 (N(*C*H$_3$)$_2$), 27.1 (*C*H$_2$), 24.6 (*C*H$_2$). δ_{7Li} (156 MHz, D_8-toluene, 30 °C): δ 0.80. δ_{7Li} (156 MHz, D_8-toluene, −80 °C): δ 1.26, 0.97, 0.64, 0.50. Anal. found: C 58.1, H 10.2, 16.1%; requires for $C_{21}H_{44}Li_2N_5O_2$: C 61.2, H 10.8, N 17.0%.

Crystallographic data for **2**. $C_{42}H_{88}Li_4N_{10}O_4$, M = 824.98, colourless prismatic, 0.20 × 0.15 × 0.11 mm, monoclinic, space group $P2_1/n$ (No. 14), a = 10.061(2), b = 14.802(3), c = 17.141(3) Å, β = 90.52(3)°, V = 2552.6(9) Å^3, Z = 2, D_c = 1.073 g cm^{-3}, F_{000} = 908, Nonius Kappa CCD, MoKα radiation, λ = 0.71073 Å, T = 123(2) K, $2\theta_{max}$ = 50.0°, 19 631 reflections collected, 4484 unique (R_{int} = 0.1284). Final GooF = 1.037, R_1 = 0.0722, wR_2 = 0.1731, R indices based on 2494 reflections with $I > 2\sigma(I)$ (refinement on F^2), 284 parameters, 0 restraints. Lp and absorption corrections applied, μ = 0.068 mm^{-1}.

[R_6–μ^6-O–Li_8·(pyr)$_2$], 3. ^{t}BuLi (1.18 ml, 1.7 M, 2.0 mmol) was added dropwise to a stirring solution of *o*-methylvalerolactim (0.23 g, 2.0 mmol) in thf (10 ml) at −78 °C under an Ar atmosphere, giving a light yellow coloured solution as it warmed slowly to −20 °C. At this point the solution was removed from the N_2/acetone cold bath and allowed to warm to rt. Pyridine (0.16 ml, 2.0 mmol) was then added slowly to the solution at 0 °C and allowed to stir for 30 min and warm to rt. During this time the solution became orange in colour. All volatiles were removed *in vacuo* leaving an orange oil, which was solubilised in hexane (5 ml). The light orange solution was stored at rt over one week, resulting in the deposition of clear cubic crystals from a dark red oil. Yield 0.10 g, 24%. δ_H (400 MHz, C_6D_6, 30 °C): δ 8.57 (2H, d, $^3J_{HH}$: 4.1 Hz, pyr-*H*), 6.99 (1H, m, pyr-*H*), 6.73 (2H, m, pyr-*H*), 3.59 (2H, br s, C*H*$_2$N), 3.56 (1H, br s, C(OCH$_3$)=C*H*), 3.51 (3H, br s, OC*H*$_3$), 2.58 (2H, br s, C*H*$_2$CH=C), 1.77 (2H, br s, CH$_2$C*H*$_2$CH$_2$). δ_C (100 MHz, C_6D_6, 30 °C): δ 167.4 (*C*(OCH$_3$)=CH), 150.5 (pyr-*C*1), 136.6 (pyr-*C*3), 124.2 (pyr-*C*2), 73.1 (C(OCH$_3$)=*C*H), 53.5 (O*C*H$_3$), 45.3 (*C*H$_2$N), 26.9 (CH$_2$*C*H$_2$CH$_2$), 24.4 (CH$_2$CH$_2$*C*H$_2$).

Crystallographic data for **3**. $C_{46}H_{70}Li_8N_8O_7$, M = 902.62, prismatic colourless, 0.12 × 0.10 × 0.08 mm, triclinic, space group $P\bar{1}$ (No. 2), a = 10.745(2), b = 11.472(2), c = 12.207(2) Å, α = 69.40(3)°, β = 64.82(3)°, γ = 82.48(3)°, V = 1274.3(4) Å^3, Z = 1, D_c = 1.176 g cm^{-3}, F_{000} = 482, Nonius Kappa CCD, MoKα radiation, λ = 0.71073 Å, T = 123(2) K, $2\theta_{max}$ = 50.0°, 16 315 reflections collected, 4470 unique (R_{int} = 0.1158). Final GooF = 1.027, R_1 = 0.0703, wR_2 = 0.1709, R indices based on 3237 reflections with $I > 2\sigma(I)$ (refinement on F^2), 316 parameters, 0 restraints. Lp and absorption corrections applied, μ = 0.077 mm^{-1}.

[R(CH$_2$=CHO)$_2$Li$_3$·pmdta]$_2$, 4. ^{n}BuLi (1.25 ml, 1.6 M, 2.0 mmol) was added dropwise to a stirring solution of *o*-methylvalerolactim (0.23 g, 2.0 mmol) in thf (10 ml) at −78 °C under an Ar atmosphere, gradually changing to a light yellow colour as it warmed up to −20 °C. At this point the solution was removed from the N_2/acetone cold bath and allowed to warm up to rt. PMDTA (0.42 ml, 2.0 mmol) was then added slowly to the solution at 0 °C and allowed to stir for 30 min and warm up to rt. During this time it changed to a darker yellow colour. Thf was removed *in vacuo* yielding a viscous orange oil, which following some gentle heating was solubilised in hexane (5 ml). The orange solution was stored at −24 °C over three weeks, which resulted in the deposition of colourless needle-like crystals. Yield 0.24 g, 41%. δ_H (300 MHz, C_6D_6, 30 °C): δ 7.57 (2H, br s, C*H*=CH$_2$), 4.21 (2H, d, $^3J_{HH}$: 13.8 Hz, CH=C*H*$_2^{trans}$), 3.80 (2H, br s, CH=C*H*$_2^{cis}$), 3.62 (3H, s, OC*H*$_3$), 3.53 (2H, br s, C*H*$_2$N), 3.46 (1H, t, $^3J_{HH}$: 5.8Hz, C=(OCH$_3$)C*H*), 2.90 (2H, br s, C*H*$_2$CH=C), 2.15 (8H, s, N(C*H*$_2$)$_2$), 2.10 (15H, s, C*H*$_3$N), 1.93 (2H, m, CH$_2$C*H*$_2$CH$_2$). δ_C (100 MHz, C_6D_6, 30 °C): δ 169.1 (*C*(OCH$_3$)), 161.1 (O*C*HCH$_2$), 74.2 (OCH*C*H$_2$), 62.8 (*C*H=C(OCH$_3$)N), 58.1 ((CH$_3$)$_2$N*C*H$_2$), 56.4 (*C*H$_2$N(CH$_3$)), 53.0 (O*C*H$_3$), 49.6 (*C*H$_2$CH$_2$CH$_2$), 46.3 ((*C*H$_3$)$_2$NCH$_2$), 43.7 (CH$_2$N(*C*H$_3$)), 27.8 (*C*H$_2$CH$_2$CH$_2$), 25.4 (CH$_2$CH$_2$*C*H$_2$).

Crystallographic data for **4**. $C_{19}H_{38}Li_3N_4O_3$, M = 391.35, colourless prismatic, 0.13 × 0.08 × 0.08 mm, monoclinic, space group $C2/c$ (No. 15), a = 20.235(4), b = 15.067(3), c = 18.853(4) Å, β = 109.41(3)°, V = 5421.2(19) Å^3, Z = 8, D_c = 0.959 g cm^{-3}, F_{000} = 1704, Nonius Kappa CCD, MoKα radiation, λ = 0.71073 Å, T = 123(2) K, $2\theta_{max}$ = 55.0°, 28 261 reflections collected, 6206 unique (R_{int} = 0.0496). Final GooF = 1.036, R_1 = 0.052, wR_2 = 0.129, R indices based on 3803 reflections with $I > 2\sigma(I)$ (refinement on F^2), 278 parameters, 2 restraints. Lp and absorption corrections applied, μ = 0.063 mm^{-1}.

C18 and C19 of the ethylene group were disordered over two positions with refined occupancies of 69 : 31%, due to this disorder the O–C and C=C bond lengths were fixed. The hexane lattice solvent molecule is also disordered over two positions with refined occupancies of 63 : 27% again each of the C–C bond distances were fixed.

[RNa·tmeda]$_2$, 5. A beige suspension of ^{n}BuNa (0.2 g, 2.5 mmol) in hexane (10 ml) was sonicated for 20 min. *o*-Methylvalerolactim (0.28 g, 2.5 mmol) was added dropwise to the stirring suspension at 0 °C. The suspension changed to a

yellow colour as it stirred at rt for 45 min. Tmeda (0.37 ml, 2.5 mmol) was added slowly leading to the dissolution of the precipitate and the formation of a slightly cloudy yellow solution. The solution was filtered *via* cannula and stored at 2 °C overnight resulting in the deposition of pale yellow needle crystals. Yield 0.52 g, 82%. Mp 91–92 °C. δ_H (400 MHz, C_6D_6, 30 °C): δ 3.70 (2H, t, $^3J_{HH}$: 4.9 Hz, CH_2N), 3.54 (3H, s, OCH_3), 3.29 (1H, t, $^3J_{HH}$: 3.4 Hz, C(OCH$_3$)=CH), 2.80 (2H, m, CH_2CH=C), 2.45 (12H, s, (CH_3)$_2$N), 2.18 (4H, s, (CH_2)$_2$N), 1.97 (2H, m, CH$_2$CH_2CH$_2$). δ_C (100 MHz, C_6D_6, 30 °C): δ 168.3 (*C*(OCH$_3$)=CH), 104.1 (C(OCH$_3$)=*C*H), 57.1 ((*C*H$_2$)$_2$N), 52.4 (O*C*H$_3$), 49.6 (*C*H$_2$N), 45.2 ((*C*H$_3$)$_2$N), 27.0 (*C*H$_2$), 24.3 (*C*H$_2$). Anal. found: C 55.1, H 10.0, 15.9%; required for $C_{12}H_{26}N_3Na_1O_1$: C 57.3, H 10.4, N 16.7%.

Crystallographic data for **5**. $C_{24}H_{52}N_6Na_2O_2$, M = 502.70, colourless prismatic, 0.20 × 0.10 × 0.10 mm, monoclinic, space group $P2_1/n$ (No. 14), a = 10.320(2), b = 19.468(4), c = 15.943(3) Å, β = 107.89(3)°, V = 3048.3(11) Å^3, Z = 4, D_c = 1.095 g cm^{-3}, F_{000} = 1104, Bruker X8 APEX CCD, MoKα radiation, λ = 0.71073 Å, T = 123(2) K, $2\theta_{max}$ = 50.0°, 27 362 reflections collected, 5358 unique (R_{int} = 0.0332). Final GooF = 1.023, R_1 = 0.0669, wR_2 = 0.1888, R indices based on 4150 reflections with $I > 2\sigma(I)$ (refinement on F^2), 317 parameters, 0 restraints. Lp and absorption corrections applied, μ = 0.095 mm^{-1}.

[R$_4$(MeO)KLi·tmeda]$_4$, 6. *o*-Methylvalerolactim (0.59 g, 5.2 mmol) was added slowly to a stirring suspension of ^{n}BuK (0.5 g, 5.2 mmol) in hexane (10 ml) at −60 °C, and allowed to warm to rt over 2 h. Tmeda (2.34 ml, 15.6 mmol) was then added to the dark red suspension and the reaction left to stir for 30 min. The reaction mixture was filtered *via* cannula and the solvent reduced *in vacuo* by *ca.* 50%. The red solution was stored at 2 °C and over five days a small crop of cubic orange crystals deposited. Yield 0.38 g, 12%.

Crystallographic data for **6**. $C_{52}H_{116}K_4Li_4N_{12}O_8$, M = 1221.73, orange cubic, 0.16 × 0.12 × 0.10 mm, orthorhombic, space group *Pbcn* (No. 60), a = 19.661(4), b = 21.434(4), c = 17.180(3) Å, V = 7240(2) Å^3, Z = 4, D_c = 1.121 g cm^{-3}, F_{000} = 2656, Nonius Kappa CCD, MoKα radiation, λ = 0.71073 Å, T = 123(2) K, $2\theta_{max}$ = 50.0°, 55 794 reflections collected, 6384 unique (R_{int} = 0.0946). Final GooF = 1.033, R_1 = 0.0802, wR_2 = 0.2077, R indices based on 3759 reflections with $I > 2\sigma(I)$ (refinement on F^2), 375 parameters, 15 restraints. Lp and absorption corrections applied, μ = 0.297 mm^{-1}.

Lithiation of *o*-methylvalerolactim in the absence of a Lewis donor

^{t}BuLi (2.4 ml, 1.7 M, 4.0 mmol) was added slowly to a stirring solution of *o*-methylvalerolactim (0.45 g, 4.0 mmol) in hexane (10 ml) at −78 °C. The reaction was allowed to warm slowly to room temperature over 30 min resulting in the formation of a yellow precipitate. The reaction was filtered *via* cannula and the precipitate washed with chilled hexane and dried *in vacuo* and stored in an Ar filled glovebox. Yield, 0.35 g. δ_H (400 MHz, C_6D_6, 30 °C): δ 3.66 (3H, s, OCH_3), 3.62 (2.9H, t, $^3J_{HH}$: 6.0 Hz, CH_2N), 3.45 (2H, m, CH_2N), 1.94 (2H, t, $^3J_{HH}$: 6.7 Hz, N=C(OCH$_3$)CH_2), 1.83 (2.8H, t, 6.5 Hz, N=C(C(CH$_3$)$_3$)CH_2), 1.36 (2.9H, m, CH_2), 1.27 (5H, m, CH_2), 1.19 (2H, m, CH_2), 1.14 (9H, br s, C(CH_3)$_3$). δ_C (100 MHz, C_6D_6, 30 °C): δ 178.8 (N=*C*(C(CH$_3$)$_3$)CH$_2$), 59.5 (O*C*H$_3$), 49.8 (*C*H$_2$N), 47.6 (*C*H$_2$N), 41.3 (*C*(CH$_3$)$_3$), 28.6 (C(*C*H$_3$)$_3$), 24.4 (*C*H$_2$), 23.2 (*C*H$_2$), 22.7 (*C*H$_2$), 21.3 (*C*H$_2$), 20.7 (*C*H$_2$), 19.2 (*C*H$_2$).

^{t}BuLi (2.4 ml, 1.7 M, 4 mmol) was added slowly to a stirring solution of *o*-methylvalerolactim (0.45 g, 4 mmol) in hexane (10 ml) at −78 °C. The reaction was allowed to warm up slowly to room temperature over 4.5 h resulting in the formation of a yellow precipitate. The reaction was filtered *via* cannula and the precipitate washed with chilled hexane and dried *in vacuo*. Yield 0.32 g. δ_H (400 MHz, C_6D_6, 30 °C): δ 4.54 (0.25H, br s, C(OCH$_3$)=CH), 3.61 (2H, br s, CH_2N), 3.53 (0.75H, br s, O(CH_3)), 3.44 (0.5H, br s, CH_2N), 2.65 (0.5H, br s, CH_2CH=C), 1.89 (0.5H, br s, CH_2CH$_2$CH=C), 1.77 (2H, br s, C((CH$_3$)$_3$CH_2)), 1.26 (4H, CH$_2$CH_2CH_2), 1.10 (9H, br s, C(CH_3)$_3$). δ_C (100 MHz, C_6D_6, 30 °C): δ 175.8 (N=*C*(C(CH$_3$)$_3$CH$_2$)), 165.7 (*C*(OCH$_3$)=CH), 113.6 (C(OCH$_3$)*C*H) 56.3 (O*C*H$_3$), 49.3 (*C*H$_2$N), 48.5 (*C*H$_2$N), 40.2 (*C*(CH$_3$)$_3$), 28.7 (C(*C*H$_3$)$_3$), 25.8 (*C*H$_2$), 24.6 (*C*H$_2$), 23.3 (*C*H$_2$), 22.3 (*C*H$_2$), 20.1 (*C*H$_2$).

Following ^{1}H-NMR analysis, the solid was transferred to a Schlenk and hexane (10 ml) added. The reaction was quenched with H_2O and the product extracted using Et_2O (3 × 10 ml). The organic layer was dried over $MgSO_4$ and concentrated *in vacuo* yielding a pale yellow oil. Yield 0.44 g. δ_H (400 MHz, C_6D_6, 30 °C): δ 3.60 (0.75H, s, OCH_3), 3.56 (2H, m, CH_2N), 3.46 (0.5H, m, CH_2'N), 2.20–2.09 (2.5H, m, N=C(OCH$_3$)CH_2), (C(C(CH$_3$)$_3$)CH_2), 1.78–1.39 (5H, m, CH_2), 1.07 (9H, s, C(CH_3)$_3$). δ_C (100 MHz, C_6D_6, 30 °C): δ 176.7 (N=*C*(C(CH$_3$)$_3$)CH$_2$), 165.3 (*C*(OCH$_3$)=CH), 102.3 (C(OCH$_3$)=*C*H), 52.0 (O*C*H$_3$), 49.5 (*C*H$_2$N), 47.0 (*C*H$_2$N), 39.7 (*C*(CH$_3$)$_3$), 28.2 (C(*C*H$_3$)$_3$), 26.0 (*C*H$_2$), 24.4 (*C*H$_2$), 22.8 (*C*H$_2$), 22.1 (*C*H$_2$), 20.0 (*C*H$_2$).

Acknowledgements

We thank the Australian Research Council and Monash University for financial support, and Dr Jonathan MacLellan for valuable input into the X-ray crystallography. PCA thanks the Royal Society of Chemistry for an International Authors Travel Grant.

References

1 M. G. A. Shvekhgeimer, *Chem. Heterocycl. Compd.*, 2005, **41**, 551.
2 P. Cledera, J. Domingo Sanchez, E. Caballero, T. Yates, E. G. Ramirez, C. Avendano, M. T. Ramos and J. C. Menendez, *Synthesis*, 2007, 3390–3398.
3 Y. Cheng, Z. Huang and M. Wang, *Curr. Org. Chem.*, 2004, **8**, 325–351.
4 B. M. Trost and R. A. Kunz, *J. Am. Chem. Soc.*, 1975, **97**, 7152.
5 C. A. Zezza, M. B. Smith, B. A. Ross, A. Arhin and P. L. E. Cronin, *J. Org. Chem.*, 1984, **49**, 4397.
6 P. J. M. Taylor, S. D. Bull and P. C. Andrews, *Synlett*, 2006, 1347.
7 D. Seebach, W. Bauer, J. Hansen, T. Laube, W. B. Schweizer and J. D. Dunitz, *J. Chem. Soc., Chem. Commun.*, 1984, 853.
8 P. C. Andrews, M. Maguire and E. Pombo-Villar, *Helv. Chim. Acta*, 2002, **85**, 3516.
9 I. Haiduc, *Organometallics*, 2004, **23**, 3.

10 R. R. Fraser and T. S. Mansour, *Tetrahedron Lett.*, 1986, **27**, 331–334.
11 E. Kuliszewska, M. Hanbauer and F. Hammerschmidt, *Chem.–Eur. J.*, 2008, **14**, 8603–8614.
12 M. P. Bernstein, F. E. Romesberg, D. J. Fuller, A. T. Harrison, D. B. Collum, Q.-Y. Liu and P. G. Williard, *J. Am. Chem. Soc.*, 1992, **114**, 5100.
13 A. E. H. Wheatley, *Chem. Soc. Rev.*, 2001, **30**, 265–273.
14 W. Clegg, L. Horsburgh, P. R. Dennison, F. M. Mackenzie and R. E. Mulvey, *Chem. Commun.*, 1996, 1065–1066.
15 T. Chivers, A. Downard and G. P. A. Yap, *J. Chem. Soc., Dalton Trans.*, 1998, 2603–2605.
16 P. C. Andrews, M. Koutsaplis and E. G. Robertson, *Organometallics*, 2009, **28**, 1697–1704.
17 K. Gregory, P. R. Schleyer and R. Snaith, *Adv. Inorg. Chem.*, 1991, **37**, 47.
18 P. C. Andrews, P. J. Duggan, G. D. Fallon, T. D. McCarthy and A. C. Peatt, *J. Chem. Soc., Dalton Trans.*, 2000, 1937.
19 P. C. Andrews, P. J. Duggan, M. Maguire and P. J. Nichols, *Chem. Commun.*, 2001, 53.
20 V. H. Gessner, C. Daschlein and C. Strohmann, *Chem.–Eur. J.*, 2009, **15**, 3320–3334.
21 J. Clayden, *Organolithiums: Selectivity for Synthesis*, Pergamon, Oxford, 2002.
22 M. Schlosser, in *Organometallics in Synthesis: A Manual*, ed. M. Schlosser, John Wiley & Sons Ltd., West Sussex, 2002, pp. 1–352.
23 R. Lehmann and M. Schlosser, *Tetrahedron Lett.*, 1984, **25**, 745–748.
24 L. Lochmann, J. Pospisil and D. Lim, *Tetrahedron Lett.*, 1966, **7**, 257.
25 A. J. Edwards, S. Hockey, F. S. Mair, P. R. Raithby and R. Snaith, *J. Org. Chem.*, 1993, **58**, 6942.
26 P. C. Andrews, M. Minopoulos and E. G. Robertson, *Eur. J. Inorg. Chem.*, 2006, 2865.
27 K. Ruhlandt-Senge, K. W. Henderson and P. C. Andrews, in *Comprehensive Organometallic Chemistry III*, ed. K. Meyer, Elsevier, Amsterdam, 2007, vol. 1, pp. 1–65.
28 T. Maetzke and D. Seebach, *Organometallics*, 1990, **9**, 3032.
29 D. Enders, D. Bachstadter, K. A. M. Kremer, M. Marsch, K. Harms and G. Boche, *Angew. Chem., Int. Ed. Engl.*, 1988, **27**, 1522.
30 K. L. Brown, L. Damm, J. D. Dunitz, A. Eschenmoser, R. Hobi and C. Kratky, *Helv. Chim. Acta*, 1978, **61**, 3108.
31 R. E. Mulvey, *Chem. Soc. Rev.*, 1991, **20**, 167.
32 Y. Tang, L. N. Zakharov, A. L. Rheingold and R. A. Kemp, *Polyhedron*, 2005, **24**, 1739–1748.
33 K. Gregory, M. Bremer, W. Bauer, P. v. R. Schleyer, N. P. Lorenzen, J. Kopf and E. Weiss, *Organometallics*, 1990, **9**, 1485–1492.
34 H. Noth, S. Rojas-Lima and A. Troll, *Eur. J. Inorg. Chem.*, 2005, 1895.
35 A. Sekiguchi and S. Tanaka, *J. Am. Chem. Soc.*, 2003, **125**, 12684.
36 J. L. Rutherford and D. B. Collum, *J. Am. Chem. Soc.*, 1999, **121**, 10198–10202.
37 G. Muller and T. Schatzle, *Z. Naturforsch., B: Chem. Sci.*, 2004, **59**, 1400–1410.
38 F. Haftbaradaran, A. M. Kuchison, M. J. Katz, G. Schatte and D. B. Leznoff, *Inorg. Chem.*, 2008, **47**, 812–822.
39 P. G. Williard and M. J. Hintze, *J. Am. Chem. Soc.*, 1987, **109**, 5539–5542.
40 K. W. Henderson, D. S. Walther and P. G. Williard, *J. Am. Chem. Soc.*, 1995, **117**, 8680–8681.
41 P. C. Andrews, G. B. Deacon, C. M. Forsyth and N. M. Scott, *Angew. Chem., Int. Ed.*, 2001, **40**, 2108–2111.
42 P. C. Andrews, S. M. Calleja and M. Maguire, *J. Chem. Soc., Dalton Trans.*, 2002, 3640.
43 D. R. Baker, R. E. Mulvey, W. Clegg and P. A. O'Neil, *J. Am. Chem. Soc.*, 1993, **115**, 6472–6473.
44 R. E. Mulvey, *Chem. Soc. Rev.*, 1998, **27**, 339–346.
45 A. R. Kennedy, J. G. MacLellan and R. E. Mulvey, *Angew. Chem., Int. Ed.*, 2001, **40**, 3245.
46 D. Seyferth, *Organometallics*, 2009, **28**, 2–33.
47 F. Antolini, P. B. Hitchcock, M. F. Lappert and P. G. Merle, *Chem. Commun.*, 2000, 1301.
48 P. C. Andrews, S. M. Calleja, M. Maguire and P. J. Nichols, *Eur. J. Inorg. Chem.*, 2002, 1583.
49 M. F. Lappert, P. P. Power, A. R. Sanger and R. C. Srivastava, *Metal and Metalloid Amides*, Ellis Horwood, West Sussex, 1980.
50 D. C. Bradley, R. C. Mehrotra, I. P. Rothwell and A. Singh, *Alkoxo and Aryloxo Derivatives of Metals*, Academic Press, London, 2001.
51 W. Clegg, S. T. Liddle, A. M. Drummond, R. E. Mulvey and A. Robertson, *Chem. Commun.*, 1999, 1569.
52 P. C. Andrews, S. M. Calleja and M. Maguire, *J. Organomet. Chem.*, 2005, **690**, 4343.
53 D. R. Armstrong, D. V. Graham, A. R. Kennedy, R. E. Mulvey and C. T. O'Hara, *Chem.–Eur. J.*, 2008, **14**, 8025–8034.
54 P. B. Hitchcock, M. F. Lappert and Z.-X. Wang, *J. Chem. Soc., Dalton Trans.*, 1997, 1953–1956.
55 P. Deslongchamps, U. O. Cheriyan, A. Guida and R. J. Taillefer, *Nouv. J. Chim.*, 1977, **1**, 235.
56 D. Stalke, *Chem. Soc. Rev.*, 1998, **27**, 171.
57 G. M. Sheldrick, *SHELXS97: Program for the Solution of Crystals Structures*, University of Goettingen, Göttingen, 1997.
58 L. J. Barbour, *XSEED: A Graphical Interface for Use with the SHELXS Program Suite*, University of Missouri, Missouri, 1999.